

# Global Biogeochemical Cycles

## RESEARCH ARTICLE

10.1029/2020GB006796

### Special Section:

The Arctic: An AGU Joint  
Special Collection

### Key Points:

- Surface seawater dimethylsulfide (DMS) concentrations remain unchanged after sea ice retreat in the western Canada Basin
- Increased wind speed is a critical factor driving the enhancement of dimethylsulfide (DMS) flux after sea ice retreat at high latitudes in the Arctic Ocean
- Nutrient supply is hypothesized to significantly impact dimethylsulfide (DMS) distribution in the western Arctic Ocean

### Supporting Information:

Supporting Information may be found in the online version of this article.

### Correspondence to:

M. Zhang and J. Yan,  
[zhangmiming@tio.org.cn](mailto:zhangmiming@tio.org.cn);  
[jpyan@tio.org.cn](mailto:jpyan@tio.org.cn)




### Citation:

Zhang, M., Marandino, C. A., Yan, J., Wu, Y., Park, K., Sun, H., et al. (2021). Unravelling surface seawater DMS concentration and sea-to-air flux changes after sea ice retreat in the western Arctic Ocean. *Global Biogeochemical Cycles*, 35, e2020GB006796. <https://doi.org/10.1029/2020GB006796>

Received 20 AUG 2020

Accepted 28 MAY 2021

## Unravelling Surface Seawater DMS Concentration and Sea-To-Air Flux Changes After Sea Ice Retreat in the Western Arctic Ocean

Miming Zhang<sup>1</sup> , Christa. A. Marandino<sup>2</sup>, Jinpei Yan<sup>1</sup> , Yanfang Wu<sup>3</sup>, Keyhong Park<sup>4</sup>, Heng Sun<sup>1</sup>, Zhongyong Gao<sup>1</sup>, and Suqing Xu<sup>1</sup> 

<sup>1</sup>Key Laboratory of Global Change and Marine-Atmospheric Chemistry of Ministry of Natural Resources (MNR), Third Institute of Oceanography, Xiamen, Fujian, China, <sup>2</sup>Forschungsbereich Marine Biogeochemie, GEOMAR Helmholtz Centre for Ocean Research Kiel, Kiel, Germany, <sup>3</sup>School of Chemistry, Australian Centre for NanoMedicine and Australian Research Council (ARC) Centre of Excellence in Convergent Bio-Nano Science and Technology, The University of New South Wales, Sydney, Australia, <sup>4</sup>Division of Polar Ocean Sciences, Korea Polar Research Institute, Incheon, South Korea

**Abstract** The receding of the seasonal ice cover in the Arctic due to climate change has been predicted by models to increase climate-active biogenic trace gas emissions, specifically those of dimethylsulfide (DMS). However, insufficient DMS measurements are currently available to either support or refute this hypothesis and to fully understand the various responses of oceanic DMS in a rapidly changing Arctic Ocean environment. Here, we present high-resolution surface water DMS data collected in the summer of 2014 in combination with a suite of ancillary variables including sea ice cover, salinity, and nutrients. We show that surface seawater DMS concentrations, generally below 0.5 nmol L<sup>-1</sup>, remained unchanged in the Canada Basin after sea ice retreat probably due to insufficient nutrients supply to the upper mixed layer and resulting low primary production. Moreover, in the Chukchi shelf region, DMS concentrations decreased following a phytoplankton bloom due to the rapid depletion and slow resupply of nutrients. Although the DMS sea-to-air fluxes were not high from a global perspective, they increased by a factor of 4-fold after sea ice retreat in the Arctic Ocean high latitudes. This increase in DMS flux was mainly driven by increased wind speed. This work provides unique observations and insights on how surface seawater DMS and flux to the atmosphere may change in the future Arctic Ocean.

## 1. Introduction

The Arctic Ocean is highly influenced by climate change (Steiner et al., 2015). It has experienced rapid sea ice retreat (Maslanik et al., 2011) and increases in temperature (Steele et al., 2008), primary production (Arrigo & van Dijken, 2015; Arrigo et al., 2008), freshwater storage (Giles et al., 2012; Mauritzen, 2012; Morrison et al., 2012), Pacific water inflow (Woodgate et al., 2012), and ocean acidity (Qi et al., 2017). Climate change alters primary production and the whole marine ecosystems in the Arctic (Babin, 2020). Primary production increased by 57% between 1998 and 2018 in the Arctic Ocean (Lewis et al., 2020). The increase in primary production during the last decade (2008–2018) was likely sustained by an influx of new nutrients, while the increases reported between 1998 and 2008 resulted from sea ice loss (Lewis et al., 2020). These changes in primary production could indirectly influence by-products of biological activities, such as dimethylsulfide (DMS) and its algal precursor dimethylsulfoniopropionate (DMSP) (Stefels et al., 2007). Accordingly, a recent remote sensing study indicated that summertime DMS emissions increased at a mean rate of  $13.3 \pm 6.7$  Gg S decade<sup>-1</sup> (~33% decade<sup>-1</sup>) due to a loss of sea ice north of 70°N between 1998 and 2016 (Galí et al., 2019).

DMS has been hypothesized to affect cloud condensation nuclei (CCN) and cloud formation, and thus, regulate the Earth's radiation budget (Charlson et al., 1987), although this hypothesis is still under debate (Quinn & Bates, 2011). Nonetheless, it has been shown that Arctic sea ice melt leads to atmospheric new particle formation (Collins et al., 2017; Dall'Osto et al., 2017), for which one of the controlling factors is the release of oceanic DMS (Abbatt et al., 2019; Becagli et al., 2016; Leitch et al., 2013; Mahmood et al., 2019). The causes of the Arctic amplification (AA), a phenomenon describing how Arctic temperatures increase twice as fast as the global average, are currently debated but reasons included the loss of sea ice and changes

in cloudiness (Dai et al., 2019; He et al., 2019; Taylor et al., 2013). There is clearly an interplay between sea ice loss, cloudiness, and AA, but the driving factors and feedback signs remain to be fully understood. For example, recent findings show counterintuitive results that low lead flux (contributing heat and moisture) periods are associated with abundant boundary layer clouds, while fewer boundary layer clouds are observed for high lead flux periods (Li et al., 2020). Another recent publication outlines the so-called Arctic cloud puzzle and points to a coordinated observation campaign and special issue discussing many relevant points for AA, aerosols, and clouds (Wendisch et al., 2019) (see more information in its special issue: [https://amt.copernicus.org/articles/special.issue10\\_971.html](https://amt.copernicus.org/articles/special.issue10_971.html)). Undoubtedly, changes in seawater DMS and DMS emission should be considered in this complex system, as they inevitably affect the products of atmospheric oxidation and the corresponding formation of particles and clouds over the Arctic Ocean (Gabric et al., 2018; Quinn et al., 2009; Sharma et al., 2012).

So far, a considerable number of DMS-related studies were conducted in the Arctic (Levasseur, 2013). Nonetheless, limited DMS data collected in the Arctic Ocean is available in the Pacific Marine Environmental Laboratory (PMEL) DMS database (<https://saga.pmel.noaa.gov/dms>) and most of these investigations were conducted in the Central Arctic Ocean (Uhlig et al., 2019), Atlantic Ocean sector of the Arctic Ocean (Galí and Simó, 2010) and in the Canadian Archipelago (Jarníková et al., 2018; Lizotte et al., 2020). Some recent Arctic Ocean studies have, however, helped to shed light on atmospheric DMS (Ghahremaninezhad et al., 2017; Mungall et al., 2016; Park et al., 2018), DMS and DMSP dynamics in sea ice (Galindo et al., 2014, 2015; Gourdal et al., 2018, 2019; Park et al., 2019) and modeling climatological DMS and its impact on climate (Hayashida et al., 2017, 2020; Kim et al., 2018; Galí et al., 2019). Although previous modeling studies have predicted that DMS emissions in the Arctic Ocean will increase significantly because of the loss of summer sea ice and the increase in primary production (Browse et al., 2014; Gabric et al., 2005; Galí et al., 2019), direct evidence of this increase remains rare, as annual field measurements of surface seawater DMS before and after sea ice retreat are scarce.

The purpose of this study was to obtain a better understanding of the changes in surface seawater DMS and its sea-to-air flux ( $F_{\text{DMS}}$ ) after the summer sea ice retreat in the western Arctic Ocean. Subsequently, we tried to identify the key driving factors of the intra-annual variability in seawater DMS and  $F_{\text{DMS}}$  in order to better predict their future changes in Arctic Ocean.

## 2. Materials and Methods

### 2.1. Cruise Information

Measurements were performed on board the R/V Xue Long during the Chinese sixth Arctic Research Expedition (CHINARE) from July 28 to September 10, 2014 (Figure 1). The cruise track was composed of two legs: transect 1 (T1), from the Chukchi Sea to the Canada Basin, from July 28 to August 15, 2014; and transect 2 (T2), from the Canada Basin to the Chukchi Sea, from August 25 to September 10, 2014. Parameters such as nutrients, salinity, temperature, and fluorescence were measured at the conductivity-temperature-depth (CTD) stations along T1.

### 2.2. Underway Measurements

The surface seawater samples were continuously brought to the analysis system through the ship's seawater pump system at a depth of 4 m. Underway measurements of surface seawater DMS were performed using a custom-made purge-and-trap system coupled with gas chromatography pulsed flame photometric detection (Trace GC, Thermo Company) (Zhang & Chen, 2015). As described in Zhang et al., (2020), various DMS concentration standards (0, 2, 5, 10, 20, 50 nmol L<sup>-1</sup>) were diluted from pure liquid DMS (>99.0%, Sigma-Aldrich) in standard seawater (salinity = 35) for calibration. The measurement system allowed the collection of one seawater DMS sample every 10 min with a detection limit of 0.05 nmol L<sup>-1</sup>. One data point was obtained at every 2–3 km along the track assuming an averaged ship speed of 10 knots. Unfiltered and gravity-filtered (glass fiber filter; Whatman; 0.7 μm) seawater samples were collected for the measurements of DMSPd (dissolved) and DMSPp (see the stations in Figure S1). About 11.5 ml filtered seawater was collected directly in a glass tube (~12 ml) from a 50 ml filter tower, and 0.5 ml 10 M NaOH was added to it. The tube was sealed and kept in a 4°C dark room for degradation for at least 12 h (Zhang & Chen, 2015). It

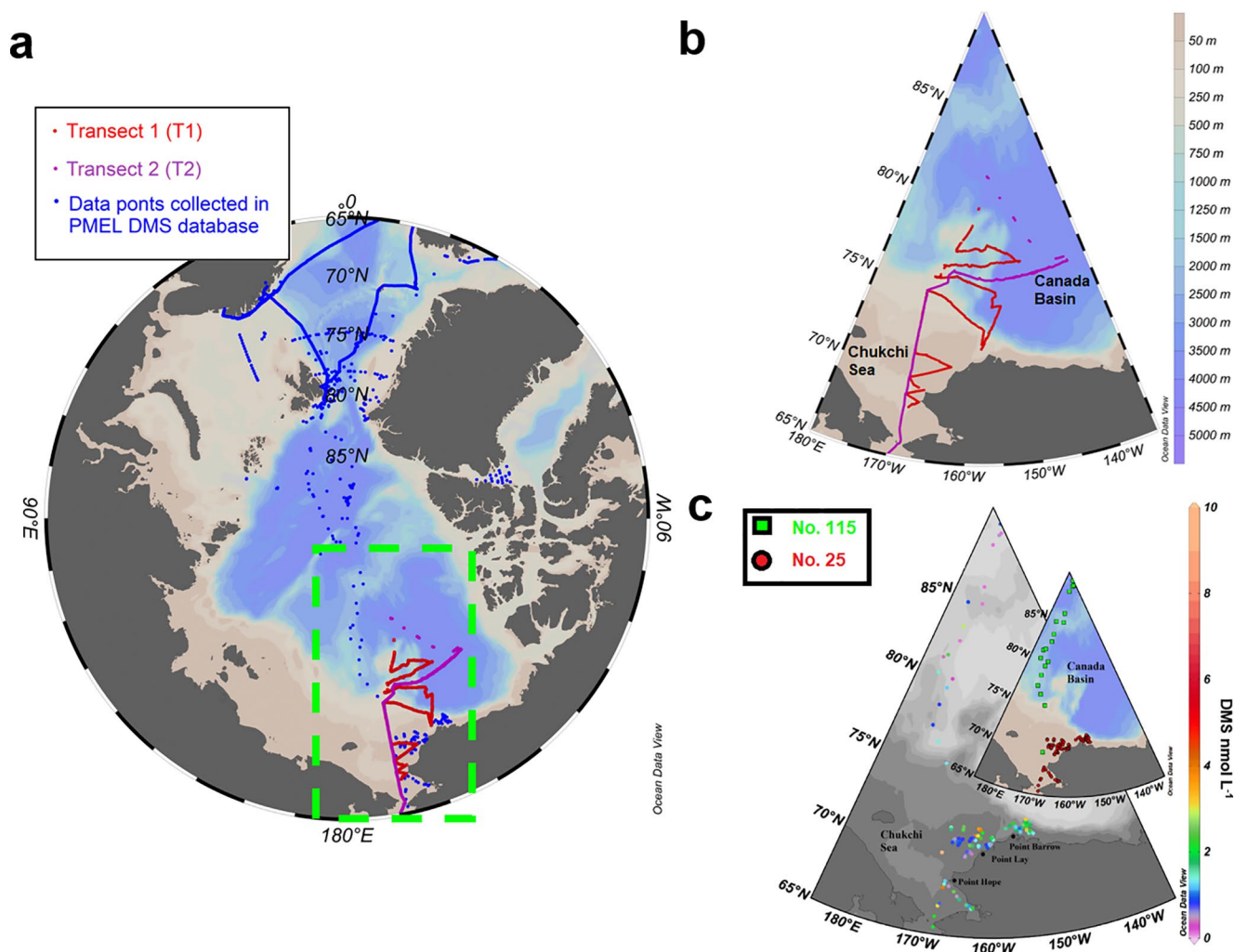


**Figure 1.** Cruise information and previous measurements in the Arctic Ocean. (a) The location of cruise tracks during the Chinese sixth Arctic Research Expedition in 2014 (dashed green box). (b) The details of cruise tracks and isobaths in the study area. Note that the Chukchi Sea and Canada Basin boundaries follow the 200–250 m isobaths. (c) Previous dimethylsulfide (DMS) data points (from the Pacific Marine Environmental Laboratory (PMEL) database) in the study area from July to September. The legend for the inset corresponds to the contribution number in the database. The references No. 115 and No. 25 are Sharma et al. (1999) and Bates et al. (1990), Bates et al. (1987), respectively.

was reported that the large volume gravity filtration method could cause cell breakage and release of DMSP (Kiene & Slezak, 2006). Therefore, our results of DMSPd measurements were possibly slightly higher than in seawater. The precision of DMSP measurements is the same as that for DMS measurements.

An automatic system (GO Flow  $p\text{CO}_2$  system, model 8050, General Oceanic Inc., Miami, FL) was installed on board for underway  $p\text{CO}_2$  measurements, and calibration was performed using  $\text{CO}_2$  standard gases from the National Oceanic and Atmospheric Administration (NOAA) with mixing ratios of 244.25, 366.86, and 546.98 ppmv ( $\text{CO}_2/\text{air}$ ) (Gao et al., 2012). Other parameters, such as the sea surface temperature (SST), salinity (SSS) and wind speed, were obtained from the shipboard underway CTD system (SBE21) or meteorological observation system (Figure S2, Figure S3). Sea ice information with a spatial resolution of 6.25 km was obtained from the University of Bremen (Spren et al., 2008) (<https://seaiice.uni-bremen.de/data/amsr2/>, Figure 2).

### 2.3. Water Column Parameters

A Rosette sampler with Niskin bottles was used to collect seawater from different depths. Nutrient samples were filtered through acid-cleaned cellulose acetate membranes (0.45  $\mu\text{m}$ ). Nitrate plus nitrite, phosphate

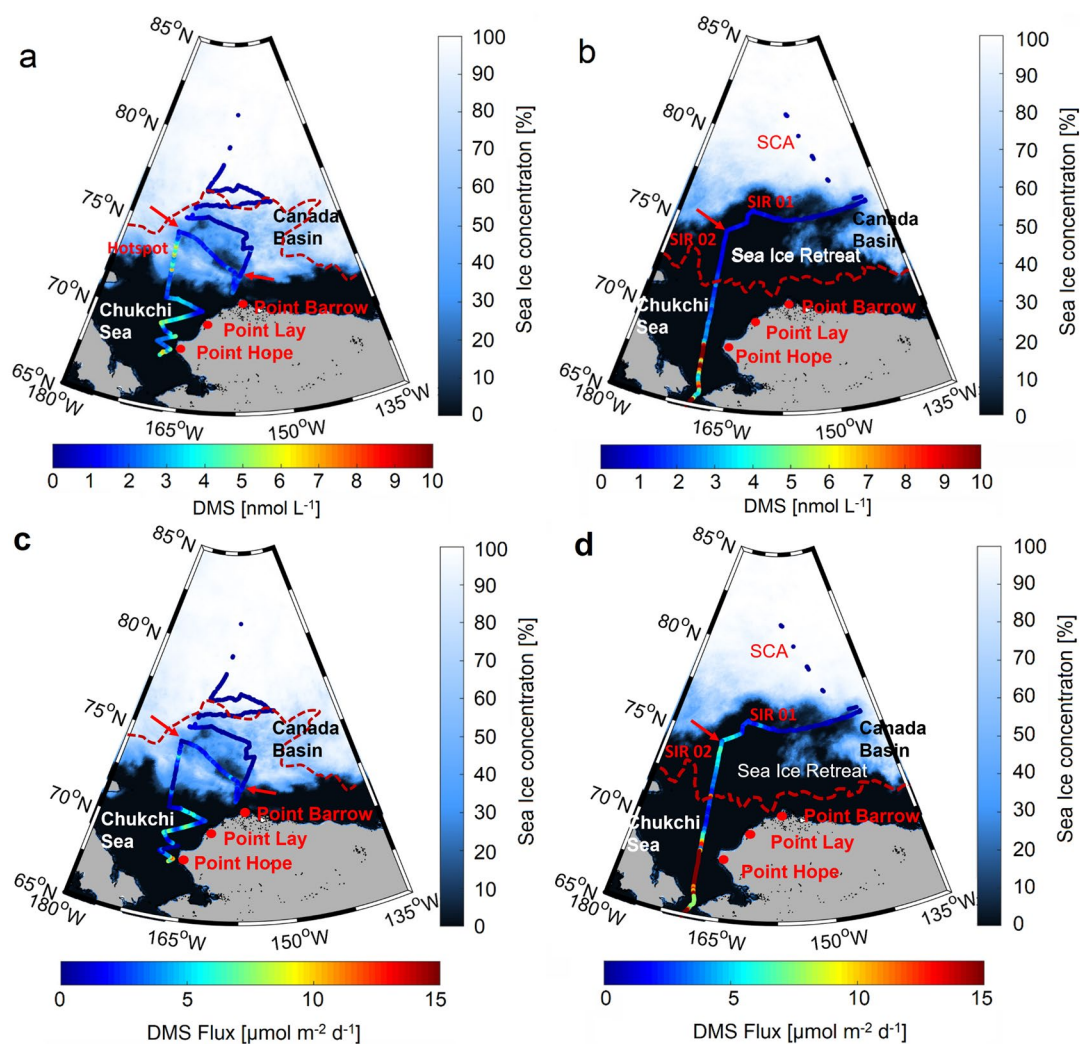


**Figure 2.** (a) and (c) Distribution of surface water dimethylsulfide (DMS) concentrations and  $F_{DMS}$  along T1. The DMS hotspot (deep red) is marked in plot (a). (b) and (d) Distribution of surface water DMS concentration and  $F_{DMS}$  along T2. Note that the sea ice cover area at high latitudes is denoted as SCA and the sea ice retreat area is denoted as SIR. These regions were divided into two parts based on the boundary of the Chukchi Sea and Canada Basin presented in Figure 1b (marked with a red arrow). Dashed red line in (a, c) and (b, d) are the sea ice edge during the period of T1 and T2 respectively. To ensure the readability of the plots, the DMS concentration and flux scales are capped at  $10 \text{ nmol L}^{-1}$  and  $15 \mu\text{mol m}^{-2} \text{ d}^{-1}$ , respectively. The white to blue background represents the mean sea ice cover during the survey.

and silicate were measured on board using a continuous flow analyzer (Skalar San++, Breda, Netherlands), and nitrite was measured using a spectrometric method (Zhuang et al., 2018). Additional parameters, such as salinity, temperature, and fluorescence, were detected by an SBE 911 plus CTD profiler and a Seapoint chlorophyll fluorometer (Sea-bird, Bellevue, Washington) attached to the CTD profiler.

#### 2.4. Sea Ice Core Sampling and Measurements

We collected five ice cores using a MARK II driller (American, i.d. 9 cm) (Figure S4). The ice cores were cut into pieces at 10 cm intervals and stored in a clean sealed container. Similar to the method in Galindo et al. (2014), the ice was allowed to slowly thaw in the sealed container at the  $4^\circ\text{C}$ . A gas-tight glass syringe was used to sample the melted water, and DMS concentrations were measured using the same method as during the underway sampling. The melting process in our protocol might introduce a slight loss of DMS from leaks in the vessel compared with the dry-crushing method or the stable isotope addition method (Stefels et al., 2012).

## 2.5. $F_{\text{DMS}}$ Calculation

The  $F_{\text{DMS}}$  was calculated as follows:

$$F = (1 - A)K(C_w - C_g/H) \quad (1)$$

where  $A$  is the fraction of sea surface covered by ice,  $K$  is the total gas transfer velocity.  $C_w$  and  $C_g$  are the seawater and air DMS concentrations, respectively. However, we did not measure the DMS concentration in air. Because the atmospheric DMS can influence the  $F_{\text{DMS}}$  calculation in polar regions (Zhang et al., 2020), we calculated the  $C_g$  as in Galí et al. (2019), where they estimated atmospheric DMS as a constant fraction of  $C_w$ ,  $C_g = C_w/252.75$  (Land et al., 2014). The Henry's law solubility is indicated as  $H$  (Dacey et al., 1984). The partitioning of the gas transfer coefficient between air-side and water-side control can change due to low SSTs and at moderate wind speeds (McGillis et al., 2000). Thus, we should consider both the water-side and air-side when calculating  $F_{\text{DMS}}$ .

$$F = (1 - A)k_w(1 - \gamma_\alpha)(C_w - C_g/H) \quad (2)$$

$$k_w = \left(0.222U_{10}^2 + 0.333U_{10}\right)(Sc_{\text{DMS}}/600)^{-1/2} \quad (3)$$

where  $k_w$  is the water-air side transfer velocity, and here we used the widely implemented empirical parameterization of Nightingale et al. (2000) as in Equation 3. The Schmidt number of DMS ( $Sc_{\text{DMS}}$ ) is a function of the SST (Saltzman & Quere, 2009); 600 is the Schmidt number of  $\text{CO}_2$  in freshwater at 25°C. 10 m wind speed is indicated by  $U_{10}$ . The atmospheric gradient fraction is indicated by  $\gamma_\alpha$  in Equation 4 (McGillis et al., 2000), indicating the partitioning between air-side and water-side control.

$$\gamma_\alpha = 1 / \left(1 + k_a/\alpha k_w\right) \quad (4)$$

where  $k_a$  is air-water side transfer coefficient and  $\alpha$  is the Ostwald solubility coefficient. These parameters were calculated as described in McGillis et al. (2000) and the references therein

$$k_a \approx 659U_{10}\left(M/M_{\text{H}_2\text{O}}\right)^{-1/2} \quad (5)$$

$$\alpha = e^{(3525/T(^{\circ}\text{K}) - 9.464)} \quad (6)$$

where  $M$  is the molecular weight of DMS or  $\text{H}_2\text{O}$  and  $T$  is the sea water temperature (K). Because the height of the wind speed measurements on the ship was approximately 27 m, we converted the wind speed into that at 10 m as follows (Hsu et al., 1994):

$$U_x / U_{10} = \left(Z_x/Z_{10}\right)^p \quad (7)$$

where  $U_x$  is the observed wind speed at 27 m,  $Z_x$  and  $Z_{10}$  are heights of 27 and 10 m, respectively, and  $p$  depends on atmospheric stability and underlying surface characteristics and is set to 0.11 (Hsu et al., 1994).

## 3. Results and Discussion

### 3.1. DMS Concentrations and $F_{\text{DMS}}$ Along the Transects in the Western Arctic Ocean

DMS concentrations decreased from the Chukchi Sea to the shelf margin and to the Canada Basin (Figure 2). The mean DMS concentrations were  $1.2 \pm 1.3 \text{ nmol L}^{-1}$  (ranging from  $0.1 \text{ nmol L}^{-1}$  to  $8.4 \text{ nmol L}^{-1}$ ,  $n = 2,285$ ) along transect 1 (T1) and  $1.4 \pm 2.4 \text{ nmol L}^{-1}$  (ranging from  $0.1 \text{ nmol L}^{-1}$  to  $17.4 \text{ nmol L}^{-1}$ ,  $n = 1,770$ ) along transect 2 (T2), respectively. The distributions of particulate DMSP (DMSPP; ranging from  $1.3 \text{ nmol L}^{-1}$  to  $33.6 \text{ nmol L}^{-1}$ ,  $n = 48$ ) and dissolved DMSP (DMSPD; ranging from  $0.3 \text{ nmol L}^{-1}$  to  $22.5 \text{ nmol L}^{-1}$ ,  $n = 49$ ) were consistent with the DMS distribution (See the DMSPP stations and relevant

DMS levels in Figure S1 and Figure S2). Strong positive correlations were found between the distributions of DMS and DMSPd ( $r^2 = 0.634$ ,  $n = 49$ ,  $p < 0.05$ ), DMS and DMSPp ( $r^2 = 0.525$ ,  $n = 48$ ,  $p < 0.05$ ) and DMS and total DMSP (DMSPt,  $r^2 = 0.576$ ,  $n = 48$ ,  $p < 0.05$ ).

Here we present the surface water DMS distribution at a much finer resolution and compared our observations with the existing data found in the PMEL database (comprising only discrete measurements, Figure 1, most of which were collected along the Alaskan coast (Bates et al., 1987; Bates et al., 1990; Sharma et al., 1999)). This comparison shows that the DMS levels measured during our cruise were higher than those previously measured in the Chukchi Sea. DMS concentrations as high as  $17.4 \text{ nmol L}^{-1}$  were observed near the Bering Strait. In contrast, north of  $76^\circ\text{N}$ , the mean value of  $0.4 \pm 0.2 \text{ nmol L}^{-1}$  ( $n = 1,159$ ) was just half the mean value of  $0.8 \pm 0.8 \text{ nmol L}^{-1}$  ( $n = 19$ ) previously measured in September–October 1985 (Bates et al., 1987; Bates et al., 1990) and July 1994 (Sharma et al., 1999), but nearly two times higher than the mean value of  $0.2 \pm 0.2 \text{ nmol L}^{-1}$  reported for August–September 2011 by Uhlig et al. (2019). These differences in DMS mean concentrations are likely because these campaigns, either ours or the previous ones, only captured one portion of the seasonal cycle.

$F_{\text{DMS}}$  varied considerably along the two cruise tracks (Figures 2c and 2d). The mean  $F_{\text{DMS}}$  along T1 and T2 were  $1.1 \pm 2.0 \text{ } \mu\text{mol m}^{-2} \text{ d}^{-1}$  ( $0\text{--}17.3 \text{ } \mu\text{mol m}^{-2} \text{ d}^{-1}$ ,  $n = 2123$ ) and  $3.5 \pm 9.2 \text{ } \mu\text{mol m}^{-2} \text{ d}^{-1}$  ( $0\text{--}69.4 \text{ } \mu\text{mol m}^{-2} \text{ d}^{-1}$ ,  $n = 1,533$ ), respectively. Strong  $F_{\text{DMS}}$  were calculated for the Chukchi Sea, whereas low  $F_{\text{DMS}}$  were calculated north of  $70^\circ\text{N}$ . This distribution pattern of  $F_{\text{DMS}}$  is consistent with the simulation results of Galí et al. (2019).  $F_{\text{DMS}}$  values from T1 in Chukchi Sea were consistent with Lana et al. (2011) climatology, while those calculated from T2 were much higher. It should be noted that our observations provide greater spatial coverage over the high latitude Arctic Ocean than included in the Lana et al. (2011) climatology. Highest  $F_{\text{DMS}}$  were found near the Bering Strait due to the high surface seawater DMS concentration ( $>10 \text{ nmol L}^{-1}$ ) and the relatively high wind speeds ( $>10 \text{ m s}^{-1}$ ). In the Canada Basin, the calculated low  $F_{\text{DMS}}$  could be explained by the low DMS concentrations ( $<0.5 \text{ nmol L}^{-1}$ ) and the presence of heavy sea ice cover.

It should be noted that other sources of DMS not investigated during our study may contribute to the DMS fluxes to the atmosphere in the ice-covered Arctic in spring. Among them, two additional sources of DMS must be considered here, melt ponds and the sea ice per se. As high DMS levels could be found in melt ponds on sea ice at high latitudes in the Arctic (Park et al., 2019), they may have contributed to DMS emissions during our expedition. A recent study found that the bottom-ice DMS could be transported upward across the ice and up to the atmosphere through the ice, with fluxes ranging between  $0.40 \text{ } \mu\text{mol m}^{-2} \text{ d}^{-1}$  and  $0.47 \text{ } \mu\text{mol m}^{-2} \text{ d}^{-1}$  through diffusion and bulk transport respectively (Gourdal et al., 2019). Thus, direct emissions through the permeable sea ice may have also contributed to the DMS fluxes during our study. Nonetheless, if we only consider the DMS emission from the open water, our high-resolution data demonstrate that the high-latitude western Arctic open ocean was a weak source of DMS during the sampling period.

As we mainly focused on the DMS release from the open ocean,  $F_{\text{DMS}}$  was computed using the surface seawater DMS concentrations and a total gas transfer velocity ( $K$ ), which is calculated using the sea ice concentration, wind speed, and SST (see Methods). This assessment was performed before and after the sea ice retreat, as this will allow us to unravel the influence of summer sea ice retreat in the Arctic in future years. In the following discussion, the data collected in the sea ice retreat area (SIR) of T2 was divided into two regions (marked in Figures 2b and 2d). One region was located in the Canada Basin (SIR 01) and the other one covered the area where a DMS hotspot occurred in T1 (SIR 02).

### 3.2. Changes in Surface Seawater DMS Levels Between the Transects

A DMS hotspot, located in the Chukchi Sea shelf break region, with concentrations reaching  $8.4 \text{ nmol L}^{-1}$  (Figure 2a), was detected in the sea ice zone ( $\sim 73^\circ\text{N}$ , sea ice concentrations generally above 50%, Figure 2a and Figure 3a), where we observed very low  $p\text{CO}_2$  levels (below  $150 \text{ } \mu\text{atm}$ ), high DMSPp and DMSPd concentrations of  $33.6 \text{ nmol L}^{-1}$  and  $22.6 \text{ nmol L}^{-1}$ , respectively (Figure S2), subsurface high nutrient levels (Figures 4d and 4e) and abundant biomass (fluorescence signal, Figure 3f). The low  $p\text{CO}_2$  levels suggest high biological uptake of  $\text{CO}_2$  (Cai et al., 2010). The sea ice was rapidly melting, indicated by the significant decrease of salinity (Figure S2), which could favor the growth of phytoplankton through releasing

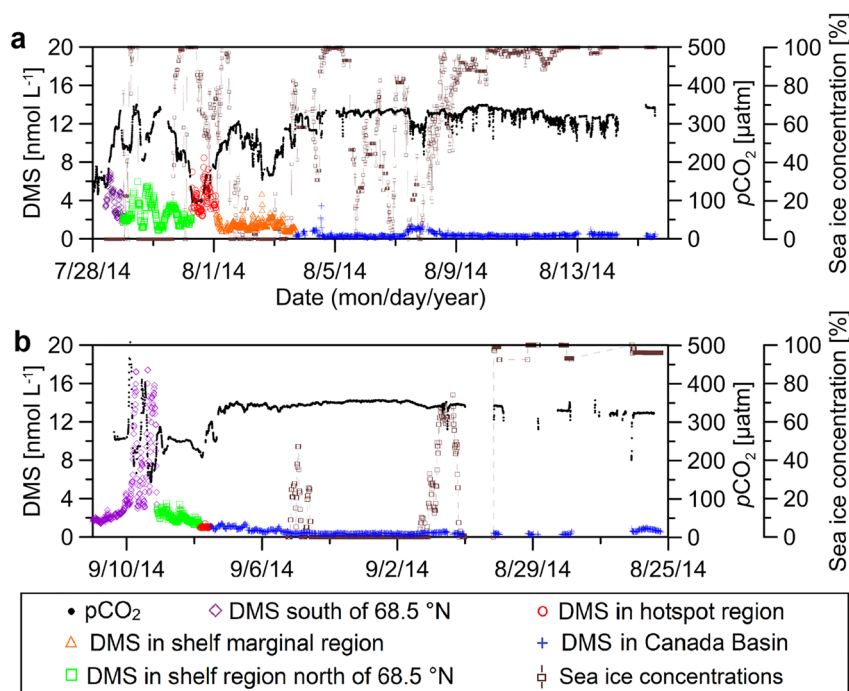


**Figure 3.** Distribution of surface seawater dimethylsulfide (DMS) concentration and  $p\text{CO}_2$ . (a) Data acquired along T1; (b) Data obtained along T2. The daily sea ice distributions along the cruise tracks are presented as well.

micro-nutrients, like iron (Wang et al., 2014). The nutrient depletion in near surface waters indicated that a phytoplankton bloom possibly occurred under the sea ice from early July (Arrigo et al., 2012). Shelf break upwelling may explain the high nutrient levels in the subsurface (Spall et al., 2014). This process persists during the winter season, producing nutrients that can be used directly during the next melt season (Tremblay et al., 2011). However, the DMS hotspot was no longer present when the ship returned in September, as the area was free of sea ice. The mean level of DMS decreased from  $3.1 \text{ nmol L}^{-1}$  to  $1.2 \text{ nmol L}^{-1}$  (SIR 02, Table 1). The  $p\text{CO}_2$  increased to above  $200 \text{ } \mu\text{atm}$ , indicating that the uptake of  $\text{CO}_2$  by phytoplankton was not as strong as during T1. Although we did not measure nutrient concentrations, phytoplankton activity and water mass physical characteristics along T2 as we did for T1, the observed low DMS concentrations could be attributed to the fact that bloom period had ceased for a relatively long time (i.e., one month had passed since the initial observation of the hotspot area) (Stefels et al., 2007). Additionally, even though the wind speed increased significantly to a mean level of  $11.2 \text{ m s}^{-1}$  after the sea ice retreat, the strong winds along with the shelf break upwelling seemed to have been insufficient at eroding the vertical stratification, bringing nutrients to upper mixed layer and stimulating primary productivity (Tremblay et al., 2011).

In the Canada Basin, the mean DMS concentration increased slightly from  $0.3 \text{ nmol L}^{-1}$  to  $0.5 \text{ nmol L}^{-1}$  in the sea ice cover area (SCA), whereas the mean DMS concentration remained unchanged ( $0.5 \text{ nmol L}^{-1}$ ) in SIR 01 (Table 1). Generally, the DMS concentrations along the cruise track remained at low levels (below  $0.5 \text{ nmol L}^{-1}$ ) and did not change after sea ice retreat (Figures 2a and 2b). We also found that DMS values remained low and constant while the  $p\text{CO}_2$  value decreased to about  $250 \text{ } \mu\text{atm}$  (Figure 3). This decrease in  $p\text{CO}_2$  was mainly related to the sea ice melting process, as the mixing of seawater with low- $\text{CO}_2$  meltwater is known to reduce  $p\text{CO}_2$  (from around  $300 \text{ } \mu\text{atm}$ ) by  $50\text{--}60 \text{ } \mu\text{atm}$  (Cai et al., 2010). This suggests that sea ice melting alone caused the observed change in the physical properties of the surface water, with no significant effect of phytoplankton productivity. Thus, our results suggest that sea ice melting had a limited influence on DMS levels at these high latitudes during our campaign. Additionally, the direct contribution of DMS from the sea ice melting to the surrounding water was also limited according to the low DMS levels we measured in the sea ice cores (Figure S4). Indeed, in contrast to the high DMS levels measured in sea ice cores, for example, DMS levels more than  $100 \text{ nmol L}^{-1}$  at the bottom of ice in Beaufort Sea in the summer (see in Levasseur, (2013) and references therein), very low DMS levels (generally below  $0.5 \text{ nmol L}^{-1}$ ) were

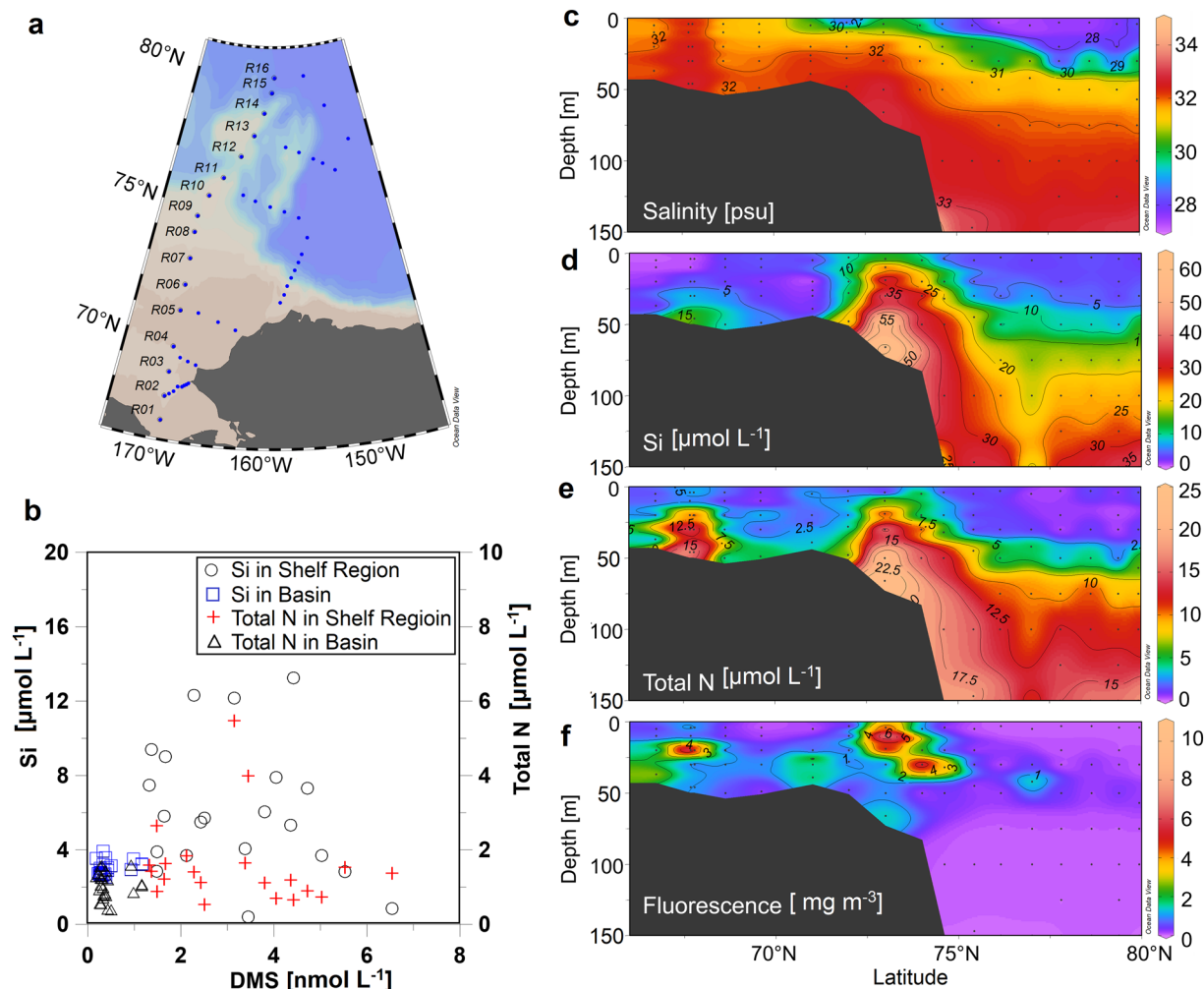


**Figure 4.** Distribution of nutrients in relation to surface seawater dimethylsulfide (DMS) in the western Arctic Ocean. (a) Locations of conductivity-temperature-depth (CTD) stations along T1. The section R, panels (c)–(f), correspond to stations labeled R on the map in (a). (b). Relationships between DMS and Si and total N in surface water of all stations in (a). The panels on the right show depth profiles of (c) salinity, (d) Si, (e) total N, and (f) fluorescence along section R.

determined in sea ice cores collected from the high latitudes during our survey (Figure S4). The concentrations of DMS precursors were low as well, DMSP<sub>p</sub> and DMSP<sub>d</sub> concentrations in the surface being generally below 3 nmol L<sup>-1</sup> and 1.5 nmol L<sup>-1</sup>, respectively (Figure S2), indicating that the potential to produce DMS from the degradation of DMSP was not strong. Additionally, the fluorescence signal indicated that algal biomass was low in the upper mixed layer in the Canada Basin (Figure 4f; Figure 5e), leading to the low surface seawater DMS and DMSP values in the Canada Basin.

In the Chukchi shelf region, the comparison of the results between the two transects indicates that the DMS levels greatly increased near 68°N and that the region of elevated DMS levels expanded northward slightly in September (Figures 2a and 2b). However, in the northern region between ~69°N and ~71°N, the DMS levels slightly decreased. Along both transects, high DMS levels coincided with low *p*CO<sub>2</sub> levels (as low as 150 μatm, Figure 3), suggesting high phytoplankton activity. Thus, the high DMS levels were possibly driven by the high phytoplankton activity. As different phytoplankton functional types produce DMSP at varying levels, the phytoplankton distribution is likely responsible for the significant temporal and spatial variability in the DMS distribution during the expedition. For instance, the relatively high DMSP<sub>p</sub> levels (~20 nM) found at the stations near Point Hope characterized by low nutrients concentrations (Mathis et al., 2007) were possibly caused by high-DMSP producers. It is well known that diatoms (the low-DMSP producers) are the main phytoplankton group in the Chukchi shelf region during summer, and that the



**Table 1**

Mean Seawater DMS, Wind Speeds, Total Transfer Velocity of DMS ( $K$ ), DMS Sea-To-Air Flux ( $F_{DMS}$ ), and Sea Ice Condition During the Two Transects in the Selected Distinct Regions

Transect	Area	Seawater DMS (nmol L <sup>-1</sup> )	Wind speeds (m s <sup>-1</sup> )	$K$ (cm h <sup>-1</sup> )	$F_{DMS}$ (μmol m <sup>-2</sup> d <sup>-1</sup> )	Sea ice condition	Note	
T1	Chukchi sea	68°N–71°S	3.1 ± 1.4 0.9–6.9	6.8 ± 1.3 4.1–9.2	6.9 ± 2.3 2.8–12.2	4.6 ± 3.1 0–17.4	Open water	
T2	Chukchi sea	64°N–71°S	5.1 ± 4.4 1.6–17.4	8.6 ± 2.7 3.4–13.9	10.7 ± 5.7 1.9–24.9	16.4 ± 18.6 1.1–69.4	Open water	Highest DMS values
T1	Chukchi Sea	SIR 02	3.1 ± 1.4 1.3–8.4	7.5 ± 1.9 2.6–11.0	7.3 ± 3.1 1.1–15.0	1.4 ± 1.5 0–7.6	cover	Hotspot
T2	Chukchi Sea	SIR 02	1.2 ± 0.3 0.8–2.1	11.2 ± 3.4 6.1–16.2	14.8 ± 6.9 5.1–26.7	4.1 ± 1.5 1.8–7.3	Retreat	▽ ▲
T1	Canada Basin	SIR 01	0.5 ± 0.4 0.1–4.3	5.1 ± 1.7 0.4–9.9	3.6 ± 1.9 0.1–10.5	0.3 ± 0.4 0–1.9	Cover	
T2	Canada Basin	SIR 01	0.5 ± 0.3 0.2–1.5	8.3 ± 3.1 0.8–13.9	8.5 ± 4.7 0.2–20.1	1.2 ± 1.1 0.01–6.7	Retreat	○ ▲
T1	Canada Basin	SCA	0.3 ± 0.1 0.2–1.0	4.4 ± 1.5 1.0–8.9	2.7 ± 1.5 0.2–8.8	0.01 ± 0.02 0–0.08	Cover	Very low values
T2	Canada Basin	SCA	0.5 ± 0.2 0.1–1.0	3.4 ± 2.3 0–8.3	2.1 ± 2.0 0–7.8	0.04 ± 0.09 0–8.0	Cover	Very low values

Note. The increase or decrease in seawater DMS after sea ice retreat is indicated by ▲ and ▼ respectively. The increase or decrease in  $F_{DMS}$  after sea ice retreat is indicated by ▲ and ▼ respectively. The symbol ○ was used to show that the DMS concentration remained unchanged after sea ice retreat. The range is shown below the corresponding mean values.

spread of the low-nutrient Alaska Coastal Current (ACC) can favor the activities of dinoflagellates and chrysophytes (high-DMSP producers) (Zhuang et al., 2016). Therefore, the different nutrient levels might affect the DMS concentrations by influencing the phytoplankton community structure.

### 3.3. Changes in $F_{DMS}$ Between the Transects

Under heavy sea ice cover conditions, calculated  $F_{DMS}$  values in the Canada Basin were very low, such as in SCA and SIR 01 (Figures 2c and 2d; Table 1). After the sea ice retreat, as expected the mean  $F_{DMS}$  increased approximately 4-fold, from 0.3 μmol m<sup>-2</sup> d<sup>-1</sup> to 1.2 μmol m<sup>-2</sup> d<sup>-1</sup>. This increase was driven by  $K$ , the mean value of which increased from 3.6 cm h<sup>-1</sup> to 8.5 cm h<sup>-1</sup> whilst the mean seawater DMS levels remained unchanged. Although the calculated  $F_{DMS}$  values were not high after sea ice retreat, a larger amount of DMS could be released into the atmosphere as the open water area increased.

In the Chukchi sea, an increase in  $F_{DMS}$  was calculated not only in the ice cover area (SIR 02), but also in the open shelf water regions. The increase was particularly important in the hotspot area of SIR 02, after the sea ice barrier was removed. In this area, the mean  $F_{DMS}$  increased from 1.4 μmol m<sup>-2</sup> d<sup>-1</sup> to 4.1 μmol m<sup>-2</sup> d<sup>-1</sup>, even though already the DMS mean concentration decreased nearly 3-fold. Similar to the fluxes in the Canada Basin, the increase in  $F_{DMS}$  could be attributed to the variations in  $K$  value. In contrast, the increase in  $F_{DMS}$  in the open water area resulted from both changes in DMS concentrations (increased from 3.1 nmol L<sup>-1</sup> to 5.1 nmol L<sup>-1</sup>) and  $K$  value (increased from 6.9 cm h<sup>-1</sup> to 10.7 cm h<sup>-1</sup>).

Besides the identified effect of the sea ice cover on  $F_{DMS}$ , we found that the variations in wind speed is another critical factor that influences the  $F_{DMS}$  in the high-latitude Arctic Ocean by affecting the  $K$  values, as expected from typical gas transfer parameterizations. We observed a slight increase in mean sea water temperature

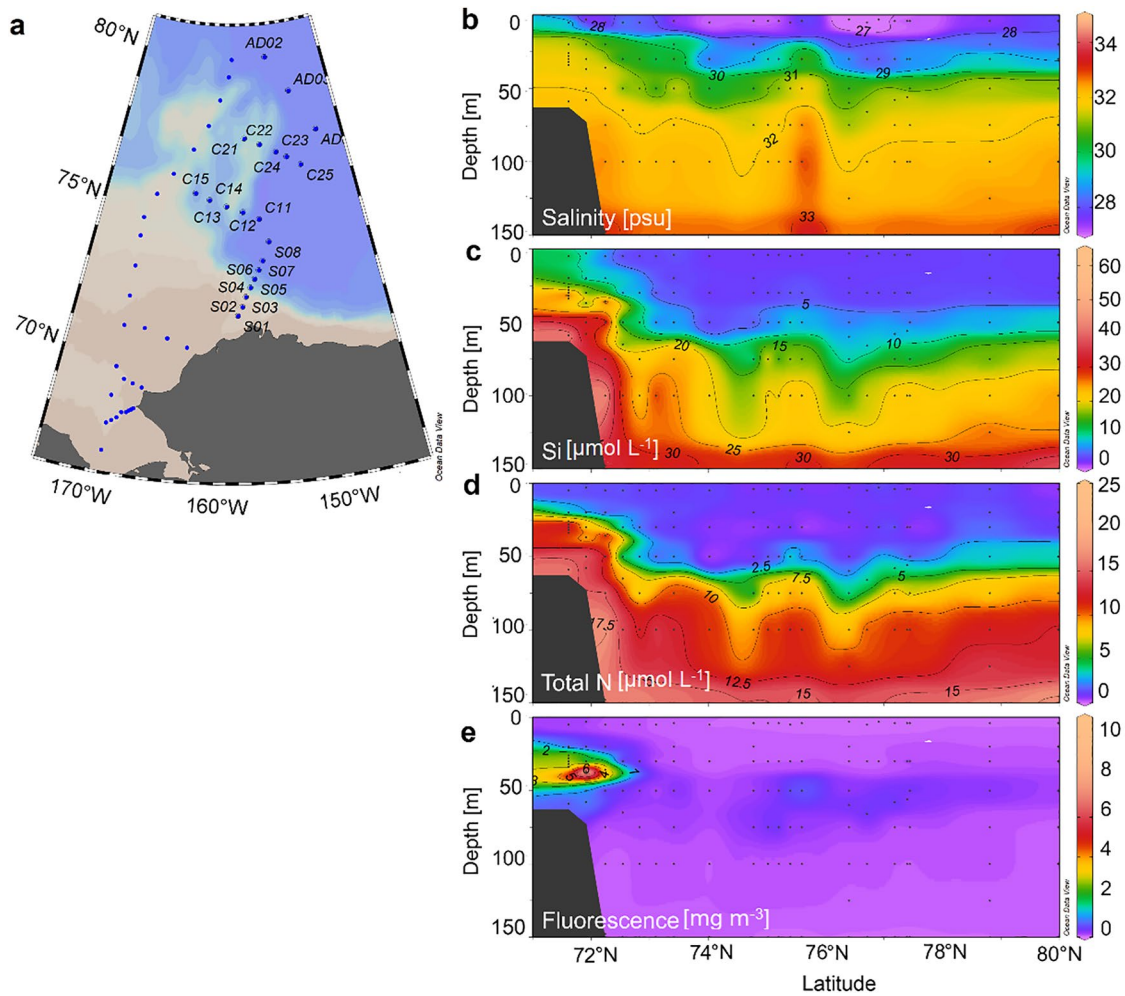


**Figure 5.** Distribution of nutrients in the Canada Basin. (a). Location of stations, indicated by their notation, used in the right panels. (b)–(e); The plots in the right panels show depth profiles of (b) salinity, (c) Si, (d) total N, and (e) fluorescence along the latitudes.

(0.26°C in the SIR 01 and 0.89°C in the SIR 02 respectively) after the sea ice retreat, resulting in a small decrease in the calculated  $Sc$  value and the atmospheric gradient fraction ( $\gamma_a$ ), and leading to a slight increase in  $K$  values. Additionally, the warming of surface water could also enhance the release of DMS via the decrease of DMS solubility (Dacey et al., 1984). However, this has little effect on the flux. Finally, the wind speed increased 2.5-fold and 2.1-fold in SIR 01 and SIR 02 respectively, causing a marked increase in  $K$  in the SIR.

In contrast to the high-latitude SIR, the mean sea water temperature in the open water area of the Chukchi Sea decreased from 7.0°C to 5.7°C, which caused a decrease in  $K$  value. Thus, the calculated increase of the  $K$  value in this region was mainly caused by changes in wind speeds (mean values varied from 6.8 m s<sup>-1</sup> to 8.6 m s<sup>-1</sup>), rather than variations in sea water temperature. Nonetheless, the decline in summer sea ice extent has been shown to increase the air-ocean exchange of momentum, moisture and heat, which enhances the strength and size of Arctic storms (Long & Perrie, 2012) and wind speed (Ardyna et al., 2014). These results stress the importance to pay more attentions to the influence of future variations in wind speed variation and their effects on oceanic DMS emissions.

### 3.4. Impact of Nutrient Supply on DMS Distribution

Although a linear relationship between DMS and nutrients was not found (Figure 4b), the comparison of their distribution highlights some interesting features. In the permanently nutrient poor regions, like in the upper

layer water of the Canada Basin (Coupel et al., 2015), low DMS and DMSP concentrations (Figure S2) were observed. The highest levels of nutrients were associated with intermediate DMS concentrations ( $2\text{--}5\text{ nmol L}^{-1}$ ), suggesting an early bloom stage. However, the highest DMS concentrations were mainly found coincidentally with low nutrients. As discussed above, this might be explained by succession of phytoplankton types, where the diatoms (low-DMSP producers) are often replaced by high-DMSP producing phytoplankton, such as dinoflagellates and chrysophytes, during post-bloom stages following when the nutrients are depleted. Another possible explanation is that there can be a temporal lag between the peak of a bloom and peak in seawater DMS. This temporal lag, often reported during previous studies, can be attributed to the time lag between DMSP release by algae and its consumption by bacteria, leading to its conversion into DMS (Simó, 2001).

In the Canada Basin, both Si and total N (sum of nitrate, nitrite and ammonium) concentrations were low in the upper layer mixed water (depth  $< 50\text{ m}$ , Si  $< 5\text{ }\mu\text{M}$ , total N  $< 2.5\text{ }\mu\text{M}$ ) (Figures 4d and 4e; Figures 5c and 5d). In addition, the salinity vertical profiles indicate that the upper mixed layer of the Canada Basin was dominated by a fresher water mass, and that the thickness of the layer (salinity  $< 30$ ) increased northward from  $\sim 10\text{ m}$  at  $\sim 74^\circ\text{N}$  (Figure 4c) and at  $\sim 72^\circ\text{N}$  (Figure 5b) to  $\sim 40\text{ m}$  at  $\sim 80^\circ\text{N}$ . These results suggest that phytoplankton growth in the Canada Basin was limited by the availability of nutrients, and that deep nutrients were not brought to the surface effectively. Following sea ice retreat, our results show no significant change in the nutrient levels in the upper layer water mass, thereby preventing phytoplankton growth (Figure 4f; Figure 5e).

Previous studies identified an increase in freshwater storage in the western Arctic Ocean, and suggested that this freshwater was prevented from leaving the Arctic Ocean by the wind-driven spin-up of the Beaufort Gyre (Giles et al., 2012; Mauritzen, 2012). Additionally, it is suggested that the enhanced eddy activity in response to sea ice loss in the western Arctic will increase the persistence of this freshwater upper layer (Armitage et al., 2020) and further limit the vertical nutrient supply from the deep ocean. Thus, although an ice-free summer in the Arctic Ocean may occur sooner than previously expected (Stroeve et al., 2007; Stroeve et al., 2012), DMS concentration may not increase significantly due to the low availability of nutrients for phytoplankton in the western Arctic Ocean basin.

The influence of nutrient depletion on DMS production in the Chukchi shelf region was also examined. Especially at the DMS hotspot ( $\sim 73^\circ\text{N}$ ), the strong decline in DMS levels between the two transects can be explained by the decrease in phytoplankton biomass attributable to nutrient depletion (Cota et al., 1996). As discussed above, the resupply of nutrients after the bloom may have been inhibited by the strong vertical stratification (Spall et al., 2014). Although nutrient-rich waters, such as the Bering Shelf Water (BSW) and Anadyr Current (AC) (Grebmeier & Mcroy, 1988) (Figure S1), pass through the Bering Strait, nutrients are rarely transported to the high latitudes due to their rapid utilization by phytoplankton in the shelf region. This process is probably responsible for the low nutrient concentrations measured between  $68.5^\circ\text{N}$  and  $74^\circ\text{N}$  (Figures 4d and 4e). In contrast, the area in the vicinity of the Bering Strait possibly maintained high biomass and associated high DMS levels during our investigation period due to an abundant supply of nutrients from the AC and BSW.

#### 4. Summary and Implications

We investigated how the levels of surface water DMS and  $F_{\text{DMS}}$  vary after sea ice retreat in western Arctic Ocean. Our results reveal that nutrient supply is an important factor affecting the surface seawater DMS concentrations. Low and stable surface seawater DMS ( $< 0.5\text{ nmol L}^{-1}$ ) before and after sea ice retreat in the Canada Basin could be attributed to low phytoplankton activity resulting from insufficient availability of nutrients due to the strong stratification characterizing the upper mixed layer of the basin. In most of the Chukchi Sea, the inefficient nutrient supply from both the Pacific inflow water and shelf break upwelling could not maintain high phytoplankton activity in the late summer, leading to a decline in surface seawater DMS levels. Additionally, although the  $F_{\text{DMS}}$  values are not high in the high latitude Arctic Ocean, enhanced  $F_{\text{DMS}}$  after sea ice retreat was calculated. Besides the loss of sea ice cover, we show that wind speed is another critical factor driving the  $F_{\text{DMS}}$  increase. Thus, enhanced storminess in the Arctic Ocean (Ardyna et al., 2014; Long & Perrie, 2012) could possibly elevate the DMS emission via increased wind speed in the future. Based on our findings, changes in primary production, nutrient availability, freshwater storage/sea ice, and surface seawater temperature have the potential to impact the seawater DMS distribution and  $F_{\text{DMS}}$ .

One should keep in mind that additional alterations of climate-related parameters such as ocean acidification could also affect DMS emissions (Six et al., 2013).

The future variability of surface water DMS is closely related to the changing primary production in the Arctic Ocean (Galí et al., 2019). The increase in primary production is caused by sea ice loss because of the increase of the surface area exposed to sunlight and the longer growth season for phytoplankton (Arrigo et al., 2008; Tremblay et al., 2015; Vancoppenolle et al., 2013). Moreover, the changes in the strength of Pacific inflow water (Corlett & Pickart, 2017; Woodgate, 2018; Woodgate et al., 2012) and of the shelf break upwelling (Spall et al., 2014; Tremblay et al., 2011) are expected to increase primary production and affect nutrient supply. The supply of new nutrients was found to be the reason for increased phytoplankton biomass, which drove the recent decadal (2009–2018) rise in Arctic Ocean primary productivity (Lewis et al., 2020). Additionally, large phytoplankton blooms beneath the sea ice can cause nutrient depletion in the early spring (Arrigo et al., 2012; Horvat et al., 2017), severely reducing the amount of nutrients available to support phytoplankton growth after the retreat of the ice cover, if the nutrient resupply is weak. Fully understanding how surface seawater DMS distributions and  $F_{\text{DMS}}$  will respond of these complex and inter-related variations will require more work in the future.

Another aspect is that DMS emissions could be enhanced by the ongoing thinning of the sea ice and the concomitant increase of melt ponds in the Arctic Ocean during the spring ice cover season (Gourdal et al., 2018; Levasseur, 2013; Park et al., 2019; Sharma et al., 1999). A recent study also indicated that DMS ventilation through permeable ice, for example, upward transport from the bottom of the sea ice through the permeable brine network ( $\sim 0.4 \mu\text{mol m}^{-2} \text{d}^{-1}$ ), could contribute DMS to atmosphere (Gourdal et al., 2019). These contributions to DMS emissions are still challenging to evaluate, as insufficient measurements of DMS in melt ponds and ice-to-air DMS flux during the spring and summer in the Arctic Ocean have been performed.

We notice that the large increase in surface seawater temperature over decades might have a potent impact on the inter-annual increase of  $F_{\text{DMS}}$ . According to the recent 2019 Arctic Report Card (Richter-Menge et al., 2019), the mean surface seawater temperature in August 2019 was about 1–7°C warmer than that of 1982–2010 August in the Beaufort and Chukchi Sea. This change in temperature might lead to an increase in  $F_{\text{DMS}}$  from 3.0% to 22.9% if we assume the other parameters, i.e., wind speed and seawater DMS levels, remain stable. Results from a study in the subpolar region indicated that the warming of the Bering Sea resulted in a significant increase in DMS, DMSP and  $F_{\text{DMS}}$  (Li et al., 2019). A warmer summer Arctic Ocean might have the same effect on both seawater DMS and  $F_{\text{DMS}}$  (Gabric et al., 2005). Therefore, the high latitude oligotrophic western Arctic Ocean, where only a small fraction of DMS emission was found (Galí et al., 2019), will possibly be altered under the warmer season.

#### Acknowledgments

The authors thank the Chinese Arctic and Antarctic Administration (CAA) of the Ministry of Natural Resources and the crew of R/V Xue Long for their support with field operations. The authors thank Prof. Jianfang Chen, Mr Yanpei Zhuang from the Second Institute of Oceanography, Ministry of Natural Resources, for providing the nutrient data. The authors also thank Prof. Maurice Levasseur from University Laval (Canada) for his valuable advice. Thanks to my wife, Mrs Jing Chen, for her kindly support. Our datasets are currently included in the Supporting Information S1 as Data set S1–S2 and will be uploaded to the PMEL repository after this paper is published. This work was supported by the Scientific Research Foundation of Third Institute of Oceanography, at the Ministry of Natural Resources (under contract No. 2019009, 2018005), the National Natural Science Foundation of China (NSFC) (41911540471, 41941014), the National key Research and Development program of China (No. 2019YFA0607003), the Chinese Projects for Investigations and Assessments of the Arctic and Antarctic (CHINARE2017–2020), the China Scholarship Council, the National Research Foundation of South Korea (NRF- 2019K2A9A2A06025329) and Korea-Arctic Ocean Warming and Response of Ecosystem project (K-AWARE, KOPRI, 1525011760).

#### Data Availability Statement

The Methods section contains the web links to the publicly available datasets used in this study. The  $p\text{CO}_2$  data set and other cruise parameters can also be downloaded from the Chinese National Arctic and Antarctic Data Center (<http://www.chinare.org.cn/data>, record number 19 on the Chinese page; please do not use the English page). The surface water DMS data set can be obtained from the Supporting Information S1. The DMS data set will also be uploaded to a publicly accessible database, like the PMEL DMS database (<http://saga.pmel.noaa.gov.dms>). For additional questions or data related to this study, please contact the corresponding author ([zhangmiming@tio.org.cn](mailto:zhangmiming@tio.org.cn)).

#### References

- Abbatt, J. P. D., Leaitch, W. R., Aliabadi, A. A., Bertram, A. K., Blanchet, J.-P., Boivin-Rioux, A., et al. (2019). Overview paper: New insights into aerosol and climate in the Arctic. *Atmospheric Chemistry and Physics*, 19(4), 2527–2560. <https://doi.org/10.5194/acp-19-2527-2019>
- Ardyna, M., Babin, M., Gosselin, M., Devred, E., Rainville, L., & Tremblay, J.-É. (2014). Recent Arctic Ocean sea ice loss triggers novel fall phytoplankton blooms. *Geophysical Research Letters*, 41(17), 6207–6212. <https://doi.org/10.1002/2014gl061047>
- Armitage, T. W. K., Manucharyan, G. E., Petty, A. A., Kwok, R., & Thompson, A. F. (2020). Enhanced eddy activity in the beaufort gyre in response to sea ice loss. *Nature Communications*, 11(1), 761. <https://doi.org/10.1038/s41467-020-14449-z>
- Arrigo, K. R., Dijken, G. V., & Pabi, S. (2008). Impact of a shrinking Arctic ice cover on marine primary production. *Geophysical Research Letters*, 35(19), 116–122. <https://doi.org/10.1029/2008GL035028>

- Arrigo, K. R., & Dijken, van, G. L. (2015). Continued increases in Arctic Ocean primary production. *Progress in Oceanography*, *136*, 60–70. <https://doi.org/10.1016/j.pocean.2015.05.002>
- Arrigo, K. R., Perovich, D. K., Pickart, R. S., Brown, Z. W., Dijken, van, G. L., Lowry, K. E., et al. (2012). Massive phytoplankton blooms under Arctic Sea ice. *Science*, *336*(6087), 1408. <https://doi.org/10.1126/science.1215065>
- Babin, M. (2020). Climate change tweaks Arctic marine ecosystems. *Science*, *369*(6500), 137–138. <https://doi.org/10.1126/science.abd1231>
- Bates, T. S., Cline, J. D., Gammon, R. H., & Kelly-Hansen, S. R. (1987). Regional and seasonal variations in the flux of oceanic dimethylsulfide to the atmosphere. *Journal of Geophysical Research*, *92*(C3), 2930–2938. <https://doi.org/10.1029/JC092iC03p02930>
- Bates, T. S., Johnson, J. E., Quinn, P. K., Goldan, P. D., Kuster, W. C., Covert, D. C., & Hahn, C. J. (1990). The biogeochemical sulfur cycle in the marine boundary layer over the northeast Pacific Ocean. *Journal of Atmospheric Chemistry*, *10*(1), 59–81. <https://doi.org/10.1007/bf01980038>
- Becagli, S., Lazzara, L., Marchese, C., Dayan, U., Ascanius, S. E., Cacciani, M., et al. (2016). Relationships linking primary production, sea ice melting, and biogenic aerosol in the Arctic. *Atmospheric Environment*, *136*, 1–15. <https://doi.org/10.1016/j.atmosenv.2016.04.002>
- Browse, J., Carslaw, K. S., Mann, G. W., Birch, C. E., Arnold, S. R., & Leck, C. (2014). The complex response of Arctic aerosol to sea-ice retreat. *Atmospheric Chemistry and Physics*, *14*, 7543–7557. <https://doi.org/10.5194/acp-14-7543-2014>
- Cai, W.-J., Chen, L., Chen, B., Gao, Z., Lee, S. H., Chen, J., et al. (2010). Decrease in the CO<sub>2</sub> uptake capacity in an ice-free Arctic Ocean basin. *Science*, *329*(5991), 556–559. <https://doi.org/10.1126/science.1189338>
- Charlson, R. J., Lovelock, J. E., Andreae, M. O., & Warren, S. G. (1987). Oceanic phytoplankton, atmospheric sulfur, cloud albedo and climate. *Nature*, *326*(6114), 655–661. <https://doi.org/10.1038/326655a0>
- Collins, D. B., Burkart, J., Chang, R. Y.-W., Lizotte, M., Boivin-Rioux, A., Blais, M., et al. (2017). Frequent ultrafine particle formation and growth in Canadian Arctic marine and coastal environments. *Atmospheric Chemistry and Physics*, *17*, 13119–13138. <https://doi.org/10.5194/acp-17-13119-2017.2017>
- Corlett, W. B., & Pickart, R. S. (2017). The Chukchi slope current. *Progress in Oceanography*, *153*, 50–65. <https://doi.org/10.1016/j.pocean.2017.04.005>
- Cota, G. F., Pomeroy, L. R., Harrison, W. G., Jones, E. P., Peters, F., Sheldon, W. M., & Weingartner, T. R. (1996). Nutrients, primary production and microbial heterotrophy in the southeastern Chukchi Sea: Arctic summer nutrient depletion and heterotrophy. *Marine Ecology Progress Series*, *135*(1–3), 247–258. <https://doi.org/10.3354/meps135247>
- Coupe, P., Ruiz-Pino, D., Sicre, M. A., Chen, J. F., Lee, S. H., Schiffrine, N., et al. (2015). The impact of freshening on phytoplankton production in the Pacific Arctic Ocean. *Progress in Oceanography*, *131*, 113–125. <https://doi.org/10.1016/j.pocean.2014.12.003>
- Dacey, J. W. H., Wakeham, S. G., & Howes, B. L. (1984). Henry's law constants for dimethylsulfide in freshwater and seawater. *Geophysical Research Letters*, *11*(10), 991–994. <https://doi.org/10.1029/GL011i010p00991>
- Dai, A., Luo, D., Song, M., & Liu, J. (2019). Arctic amplification is caused by sea-ice loss under increasing CO<sub>2</sub>. *Nature Communications*, *10*(1), 121. <https://doi.org/10.1038/s41467-018-07954-9>
- Dall'Osto, M., Beddows, D. C. S., Tunved, P., Krejci, R., Ström, J., Hansson, H.-C., et al. (2017). Arctic sea ice melt leads to atmospheric new particle formation. *Scientific Reports*, *7*(1), 3318. <https://doi.org/10.1038/s41598-017-03328-1>
- Gabric, A. J., Qu, B. O., Matrai, P., & Hirst, A. C. (2005). The simulated response of dimethylsulfide production in the Arctic Ocean to global warming. *Tellus B: Chemical and Physical Meteorology*, *57*(5), 391–403. <https://doi.org/10.1111/j.1600-0889.2005.00163.x>
- Gabric, A., Matrai, P., Jones, G., & Middleton, J. (2018). The nexus between sea ice and polar emissions of marine biogenic aerosols. *Bulletin of the American Meteorological Society*, *99*(1), 61–81. <https://doi.org/10.1175/BAMS-D-16-0254.1>
- Gali, M., Devred, E., Babin, M., & Levasseur, M. (2019). Decadal increase in Arctic dimethylsulfide emission. *Proceedings of the National Academy of Sciences*, *116*(39), 19311–19317. <https://doi.org/10.1073/pnas.1904378116>
- Gali, M., & Simó, R. (2010). Occurrence and cycling of dimethylated sulfur compounds in the Arctic during summer receding of the ice edge. *Marine Chemistry*, *122*(1–4), 105–117. <https://doi.org/10.1016/j.marchem.2010.07.003>
- Galindo, V., Levasseur, M., Mundy, C. J., Gosselin, M., Tremblay, J. É., Scarratt, M., et al. (2014). Biological and physical processes influencing sea ice, under-ice algae, and dimethylsulfoniopropionate during spring in the Canadian Arctic Archipelago. *Journal of Geophysical Research: Oceans*, *119*(6), 3746–3766. <https://doi.org/10.1002/2013JC009497>
- Galindo, V., Levasseur, M., Scarratt, M., Mundy, C. J., Gosselin, M., Kiene, R. P., et al. (2015). Under-ice microbial dimethylsulfoniopropionate metabolism during the melt period in the Canadian Arctic archipelago. *Marine Ecology Progress Series*, *524*, 39–53. <https://doi.org/10.3354/meps11144>
- Gao, Z., Chen, L., Sun, H., Chen, B., & Cai, W.-J. (2012). Distributions and air–sea fluxes of carbon dioxide in the western Arctic Ocean. *Deep Sea Research Part II: Topical Studies in Oceanography*, *81–84*, 46–52. <https://doi.org/10.1016/j.dsr2.2012.08.021>
- Ghahremaninezhad, R., Norman, A.-L., Croft, B., Martin, R. V., Pierce, J. R., Burkart, et al. (2017). Boundary layer and free-tropospheric dimethyl sulfide in the Arctic spring and summer. *Atmospheric Chemistry and Physics*, *17*, 8757–8770. <https://doi.org/10.5194/acp-17-8757-2017.2017>
- Giles, K. A., Laxon, S. W., Ridout, A. L., Wingham, D. J., & Bacon, S. (2012). Western Arctic Ocean freshwater storage increased by wind-driven spin-up of the beaufort gyre. *Nature Geoscience*, *5*(3), 194–197. <https://doi.org/10.1038/ngeo1379>
- Gourdal, M., Crabeck, O., Lizotte, M., Galindo, V., & Levasseur, M. (2019). Upward transport of bottom-ice dimethyl sulfide during advanced melting of arctic first-year sea ice. *Elementa Science of the Anthropocene*, *7*(33). <https://doi.org/10.1525/elementa.370>
- Gourdal, M., Lizotte, M., Massé, G., Gosselin, M., Poulin, M., Scarratt, M., et al. (2018). Dimethyl sulfide dynamics in first-year sea ice melt ponds in the Canadian Arctic archipelago. *Biogeosciences*, *15*(10), 3169–3188. <https://doi.org/10.5194/bg-15-3169-2018>
- Grebmeier, J., & Mcroy, C. (1988). Pelagic-benthic coupling on the shelf of the northern Bering and Chukchi Seas. III Benthic food supply and carbon cycling. *Marine Ecology Progress Series*, *48*(1), 253–268. <https://doi.org/10.3354/meps048057>
- Hayashida, H., Carnat, G., Gali, M., Monahan, A. H., Mortenson, E., Sou, T., & Steiner, N. S. (2020). Spatiotemporal variability in modeled bottom ice and sea surface dimethylsulfide concentrations and fluxes in the Arctic during 1979–2015. *Global Biogeochemical Cycles*, *34*(10), e2019GB006456. <https://doi.org/10.1029/2019GB006456>
- Hayashida, H., Steiner, N., Monahan, A., Galindo, V., Lizotte, M., & Levasseur, M. (2017). Implications of sea-ice biogeochemistry for oceanic production and emissions of dimethyl sulfide in the Arctic. *Biogeosciences*, *14*(12), 3129–3155. <https://doi.org/10.5194/bg-14-3129-2017>
- He, M., Hu, Y., Chen, N., Wang, D., Huang, J., & Starnes, K. (2019). High cloud coverage over melted areas dominates the impact of clouds on the albedo feedback in the Arctic. *Scientific Reports*, *9*(1), 9529. <https://doi.org/10.1038/s41598-019-44155-w>
- Horvat, C., Jones, D. R., Iams, S., Schroeder, D., Flocco, D., & Feltham, D. (2017). The frequency and extent of sub-ice phytoplankton blooms in the Arctic Ocean. *Science Advances*, *3*(3), e1601191. <https://doi.org/10.1126/sciadv.1601191>

- Hsu, S. A., Meindl, E. A., & Gilhousen, D. B. (1994). Determining the power-law wind-profile exponent under near-neutral stability conditions at sea. *Journal of Applied Meteorology*, 33(6), 757–765. [https://doi.org/10.1175/1520-0450\(1994\)033<0757:dtpwlp>2.0.co;2](https://doi.org/10.1175/1520-0450(1994)033<0757:dtpwlp>2.0.co;2)
- Jarníková, T., Dacey, J., Lizotte, M., Levasseur, M., & Tortell, P. (2018). The distribution of methylated sulfur compounds, DMS and DMSP, in Canadian subarctic and Arctic marine waters during summer 2015. *Biogeosciences*, 15(8), 1–51. <https://doi.org/10.5194/bg-15-2449-2018>
- Kiene, R. P., & Slezak, D. (2006). Low dissolved DMSP concentrations in seawater revealed by small-volume gravity filtration and dialysis sampling. *Limnology and Oceanography: Methods*, 4(4), 80–95. <https://doi.org/10.4319/lom.2006.4.80>
- Kim, A.-H., Yum, S. S., Lee, H., Chang, D. Y., Shim, S. (2018). Polar cooling effect due to increase of phytoplankton and dimethyl-sulfide emission. *Atmosphere*, 9, 384. <https://doi.org/10.3390/atmos9100384>
- Lana, A., Bell, T., Simó, R., Vallina, S. M., Ballabrera-Poy, J., Kettle, A., et al. (2011). An updated climatology of surface dimethylsulfide concentrations and emission fluxes in the global ocean. *Global Biogeochemical Cycles*, 25(1), GB1004. <https://doi.org/10.1029/2010GB003850>
- Land, P. E., Shutler, J. D., Bell, T. G., & Yang, M. (2014). Exploiting satellite earth observation to quantify current global oceanic DMS flux and its future climate sensitivity. *Journal of Geophysical Research: Oceans*, 119(11), 7725–7740. <https://doi.org/10.1002/2014jc010104>
- Leaith, W. R., Sharma, S., Huang, L., Toom-Sauntry, D., Chivulescu, A., Macdonald, A. M., et al. (2013). Dimethyl sulfide control of the clean summertime Arctic aerosol and cloud. *Elementa Science of Anthropocene*, 1, 000017. <https://doi.org/10.12952/journal.elementa.000017>
- Levasseur, M. (2013). Impact of Arctic meltdown on the microbial cycling of sulfur. *Nature Geoscience*, 6(9), 691–700. <https://doi.org/10.1038/ngeo1910>
- Lewis, K. M., Dijken, van, G. L., & Arrigo, K. R. (2020). Changes in phytoplankton concentration now drive increased Arctic Ocean primary production. *Science*, 369(6500), 198–202. <https://doi.org/10.1126/science.aay8380>
- Li, C.-X., Wang, B.-D., Wang, Z.-C., Li, J., Yang, G.-P., Chen, J.-F., et al. (2019). Spatial and interannual variability in distributions and cycling of summer biogenic sulfur in the bering sea. *Geophysical Research Letters*, 46(9), 4816–4825. <https://doi.org/10.1029/2018gl080446>
- Li, X., Krueger, S. K., Strong, C., Mace, G. G., & Benson, S. (2020). Midwinter Arctic leads form and dissipate low clouds. *Nature Communications*, 11(1), 206. <https://doi.org/10.1038/s41467-019-14074-5>
- Lizotte, M., Levasseur, M., Galindo, V., Gourdal, M., Gosselin, M., Tremblay, J. É., et al. (2020). Phytoplankton and dimethylsulfide dynamics at two contrasting Arctic ice edges. *Biogeosciences*, 17(6), 1557–1581. <https://doi.org/10.5194/bg-17-1557-2020>
- Long, Z., & Perrie, W. (2012). Air-sea interactions during an Arctic storm. *Journal of Geophysical Research*, 117(D15), D15103. <https://doi.org/10.1029/2011jd016985>
- Mahmood, R., Salzen, von, K., Norman, A.-L., Galí, M., & Levasseur, M. (2019). Sensitivity of Arctic sulfate aerosol and clouds to changes in future surface seawater dimethylsulfide concentrations. *Atmospheric Chemistry and Physics*, 19(9). <https://doi.org/10.5194/acp-19-6419-2019>
- Maslanik, J., Stroeve, J., Fowler, C., & Emery, W. (2011). Distribution and trends in Arctic sea ice age through spring 2011. *Geophysical Research Letters*, 38(13), L13502. <https://doi.org/10.1029/2011GL047735>
- Mathis, J. T., Pickart, R. S., Hansell, D. A., Kadko, D., & Bates, N. R. (2007). Eddy transport of organic carbon and nutrients from the Chukchi Shelf: Impact on the upper halocline of the western Arctic Ocean. *Journal of Geophysical Research*, 112(C5), C05011. <https://doi.org/10.1029/2006JC003899>
- Mauritzen, C. (2012). Oceanography Arctic freshwater. *Nature Geoscience*, 5(3), 162–164. <https://doi.org/10.1038/ngeo1409>
- McGillis, W., Dacey, J., Frew, N., Bock, E., & Nelson, R. (2000). Water-air flux of dimethylsulfide. *Journal of Geophysical Research*, 105, 1187–1193. <https://doi.org/10.1029/1999jc900243>
- Morison, J., Kwok, R., Peralta-Ferriz, C., Alkire, M., Rigor, I., Andersen, R., & Steele, M. (2012). Changing Arctic Ocean freshwater pathways. *Nature*, 481(7379), 66–70. <https://doi.org/10.1038/nature10705>
- Mungall, E. L., Croft, B., Lizotte, M., Thomas, J. L., Murphy, J. G., Levasseur, M., et al. (2016). Dimethyl sulfide in the summertime Arctic atmosphere: Measurements and source sensitivity simulations. *Atmospheric Chemistry and Physics*, 16(11), 6665–6680. <https://doi.org/10.5194/acp-16-6665-2016>
- Nightingale, P. D., Malin, G., Law, C. S., Watson, A. J., Liss, P. S., Liddicoat, M. I., et al. (2000). In situ evaluation of air-sea gas exchange parameterizations using novel conservative and volatile tracers. *Global Biogeochemical Cycles*, 14(1), 373–387. <https://doi.org/10.1029/1999GB900091>
- Park, K., Kim, I., Choi, J.-O., Lee, Y., Jung, J., Ha, S.-Y., et al. (2019). Unexpectedly high dimethyl sulfide concentration in high-latitude Arctic sea ice melt ponds. *Environmental Sciences: Processes & Impacts*, 21(2). <https://doi.org/10.1039/c9em00195f>
- Park, K.-T., Lee, K., Kim, T.-W., Yoon, Y. J., Jang, E.-H., Jang, S., et al. (2018). Atmospheric DMS in the Arctic Ocean and its relation to phytoplankton biomass. *Global Biogeochemical Cycles*, 32(3), 351–359. <https://doi.org/10.1002/2017GB005805>
- Qi, D., Chen, L., Chen, B., Gao, Z., Zhong, W., Feely, R., et al. (2017). Increase in acidifying water in the western Arctic Ocean. *Nature Climate Change*, 7, 195–199. <https://doi.org/10.1038/nclimate3228>
- Quinn, P., & Bates, T. (2011). The case against climate regulation via oceanic phytoplankton sulfur emissions. *Nature*, 480(7375), 51–56. <https://doi.org/10.1038/nature10580>
- Quinn, P. K., Bates, T. S., Schulz, K., & Shaw, G. E. (2009). Decadal trends in aerosol chemical composition at Barrow, Alaska: 1976–2008. *Atmospheric Chemistry and Physics*, 9(5), 8883–8888. <https://doi.org/10.5194/acp-9-8883-2009>
- Richter-Menge, J., Druckenmiller, M. L., & Jeffries, M. (2019). *Arctic report card 2019*. Retrieved from <https://www.arctic.noaa.gov/Report-Card>
- Saltzman, E. S., & Quere, C. L. (2009). *Surface ocean-lower atmosphere processes* (pp. 329). Washington, DC: American Geophysical Union.
- Sharma, S., Barrie, L., Plummer, D., McConnell, J., Brickell, P., Levasseur, M., et al. (1999). Flux estimation of oceanic dimethyl sulfide around North America. *Journal of Geophysical Research*, 104, 21327–21342. <https://doi.org/10.1029/1999JD900207>
- Sharma, S., Chan, E., Ishizawa, M., Sauntry, D., Gong, S. L., Li, S. M., et al. (2012). Influence of transport and ocean ice extent on biogenic aerosol sulfur in the Arctic atmosphere. *Journal of Geophysical Research*, 117(D12), D12209. <https://doi.org/10.1029/2011jd017074>
- Simó, R. (2001). Production of atmospheric sulfur by oceanic plankton: Biogeochemical, ecological and evolutionary links. *Trends in Ecology & Evolution*, 16(6), 287–294. [https://doi.org/10.1016/S0169-5347\(01\)02152-8](https://doi.org/10.1016/S0169-5347(01)02152-8)
- Six, K. D., Kloster, S., Ilyina, T., Archer, S. D., Zhang, K., & Maier-Reimer, E. (2013). Global warming amplified by reduced sulfur fluxes as a result of ocean acidification. *Nature Climate Change*, 3(11), 975–978. <https://doi.org/10.1038/NCLIMATE1981>
- Spall, M. A., Pickart, R. S., Brugler, E. T., Moore, G. W. K., Thomas, L., & Arrigo, K. R. (2014). Role of shelfbreak upwelling in the formation of a massive under-ice bloom in the Chukchi Sea. *Deep Sea Research Part II: Topical Studies in Oceanography*, 105, 17–29. <https://doi.org/10.1016/j.dsr2.2014.03.017>

- Spreen, G., Kaleschke, L., & Heygster, G. (2008). Sea ice remote sensing using AMSR-E 89-GHz channels. *Journal of Geophysical Research*, 113(C2), C02S03. <https://doi.org/10.1029/2005JC003384>
- Steele, M., Ermold, W., & Zhang, J. (2008). Arctic Ocean surface warming trends over the past 100 years. *Geophysical Research Letters*, 35(2), L02614. <https://doi.org/10.1029/2007GL031651>
- Stefels, J., Carnat, G., Dacey, J. W. H., Goossens, T., Elzenga, J. T. M., & Tison, J.-L. (2012). The analysis of dimethylsulfide and dimethylsulfoniopropionate in sea ice: Dry-crushing and melting using stable isotope additions. *Marine Chemistry*, 128–129, 34–43. <https://doi.org/10.1016/j.marchem.2011.09.007>
- Stefels, J., Steinke, M., Turner, S., Malin, G., & Belviso, S. (2007). Environmental constraints on the production and removal of the climatically active gas dimethylsulphide (DMS) and implications for ecosystem modelling. *Biogeochemistry*, 83(1), 245–275. <https://doi.org/10.1007/s10533-007-9091-5>
- Steiner, N., Azetsu-Scott, S., Hamilton, J., Hedges, K. J., Hu, X., Janjua, M. Y., et al. (2015). Observed trends and climate projections affecting marine ecosystems in the Canadian Arctic. *Environmental Reviews*, 23(2), 191–239. <https://doi.org/10.1139/er-2014-0066>
- Stroeve, J., Holland, M. M., Meier, W., Scambos, T., & Serreze, M. (2007). Arctic sea ice decline: Faster than forecast. *Geophysical Research Letters*, 34(9), L09501. <https://doi.org/10.1029/2007gl029703>
- Stroeve, J. C., Kattsov, V., Barrett, A., Serreze, M., Pavlova, T., Holland, M., & Meier, W. N. (2012). Trends in Arctic sea ice extent from CMIP5, CMIP3 and observations. *Geophysical Research Letters*, 39(16), L16502. <https://doi.org/10.1029/2012GL052676>
- Taylor, P. C., Cai, M., Hu, A., Meehl, J., Washington, W., & Zhang, G. J. (2013). A decomposition of feedback contributions to polar warming amplification. *Journal of Climate*, 26(18), 7023–7043. <https://doi.org/10.1175/jcli-d-12-00696.1>
- Tremblay, J.-É., Anderson, L. G., Matrai, P., Coupel, P., Bélanger, S., Michel, C., & Reigstad, M. (2015). Global and regional drivers of nutrient supply, primary production and CO<sub>2</sub> drawdown in the changing Arctic Ocean. *Progress in Oceanography*, 139, 171–196. <https://doi.org/10.1016/j.pocean.2015.08.009>
- Tremblay, J.-É., Belanger, S., Barber, D. G., Asplin, M., Martin, J., Darnis, G., et al. (2011). Climate forcing multiplies biological productivity in the coastal Arctic Ocean. *Geophysical Research Letters*, 38(18), L18604. <https://doi.org/10.1029/2011gl048825>
- Uhlig, C., Damm, E., Peeken, I., Krumpfen, T., Rabe, B., Korhonen, M., & Ludwichowski, K.-U. (2019). Sea ice and water mass influence dimethylsulfide concentrations in the central Arctic Ocean. *Frontiers of Earth Science*, 7(179). <https://doi.org/10.3389/feart.2019.00179>
- Vancoppenolle, M., Bopp, L., Madec, G., Dunne, J., Ilyina, T., Halloran, P. R., & Steiner, N. (2013). Future Arctic Ocean primary productivity from CMIP5 simulations: Uncertain outcome, but consistent mechanisms. *Global Biogeochemical Cycles*, 27(3), 605–619. <https://doi.org/10.1002/gbc.20055>
- Wang, S., Bailey, D., Lindsay, K., Moore, J. K., & Holland, M. (2014). Impact of sea ice on the marine iron cycle and phytoplankton productivity. *Biogeosciences*, 11(17), 4713–4731. <https://doi.org/10.5194/bg-11-4713-2014>
- Wendisch, M., Macke, A., Ehrlich, A., Lupkes, M., Mech, M., Chechin, D., et al. (2019). The Arctic cloud puzzle: Using ALOUD/PASCAL multiplatform observations to unravel the role of clouds and aerosol particles in Arctic amplification. *Bulletin of the American Meteorological Society*, 100(5), 841–871. <https://doi.org/10.1175/bams-d-18-0072.1>
- Woodgate, R. A. (2018). Increases in the Pacific inflow to the Arctic from 1990 to 2015, and insights into seasonal trends and driving mechanisms from year-round Bering Strait mooring data. *Progress in Oceanography*, 160, 124–154. <https://doi.org/10.1016/j.pocean.2017.12.007>
- Woodgate, R. A., Weingartner, T. J., & Lindsay, R. (2012). Observed increases in Bering Strait oceanic fluxes from the Pacific to the Arctic from 2001 to 2011 and their impacts on the Arctic Ocean water column. *Geophysical Research Letters*, 39(39), L24603. <https://doi.org/10.1029/2012GL054092>
- Zhang, M., & Chen, L. (2015). Continuous underway measurements of dimethyl sulfide in seawater by purge and trap gas chromatography coupled with pulsed flame photometric detection. *Marine Chemistry*, 174, 67–72. <https://doi.org/10.1016/j.marchem.2015.05.006>
- Zhang, M., Park, K.-T., Yan, J., Park, K., Wu, Y., Jang, E., et al. (2020). Atmospheric dimethyl sulfide and its significant influence on the sea-to-air flux calculation over the Southern Ocean. *Progress in Oceanography*, 186, 102392. <https://doi.org/10.1016/j.pocean.2020.102392>
- Zhuang, Y., Jin, H., Chen, J., Li, H., Ji, Z., Bai, Y., & Zhang, T. (2018). Nutrient and phytoplankton dynamics driven by the beaufort gyre in the western Arctic Ocean during the period 2008–2014. *Deep Sea Research Part I: Oceanographic Research Papers*, 137, 30–37. <https://doi.org/10.1016/j.dsr.2018.05.002>
- Zhuang, Y., Jin, H., Li, H., Chen, J., Lin, L., Bai, Y., et al. (2016). Pacific inflow control on phytoplankton community in the Eastern Chukchi Shelf during summer. *Continental Shelf Research*, 129, 23–32. <https://doi.org/10.1016/j.csr.2016.09.010>